

# Arg-302 facilitates deprotonation of Glu-325 in the transport mechanism of the lactose permease from *Escherichia coli*

Miklós Sahin-Tóth and H. Ronald Kaback\*

Howard Hughes Medical Institute, Departments of Physiology, Microbiology, and Molecular Genetics, Molecular Biology Institute, University of California, Los Angeles, CA 90095-1662

Contributed by H. Ronald Kaback, March 21, 2001

**A mechanistic model for lactose/H<sup>+</sup> symport via the lactose permease of *Escherichia coli* proposed recently indicates that the permease must be protonated to bind ligand with high affinity. Moreover, in the ground state, the symported H<sup>+</sup> is shared between His-322 (helix X) and Glu-269 (helix VIII), whereas Glu-325 (helix X) is charge-paired with Arg-302 (helix IX). Substrate binding at the outer surface induces a conformational change that leads to transfer of the H<sup>+</sup> to Glu-325 and reorientation of the binding site to the inner surface. After release of the substrate, Glu-325 is deprotonated on the inside because of rejuxtapositioning with Arg-302. To test the role of Arg-302 in the mechanism, the catalytic properties of mutants Arg-302→Ala and Arg-302→Ser were studied. Both mutants are severely defective in active lactose transport, as well as in efflux or influx down a concentration gradient, translocation modes that involve net H<sup>+</sup> movement. In marked contrast, the mutants catalyze equilibrium exchange of lactose and bind ligand with high affinity. These characteristics are remarkably analogous to those of permease mutants with neutral replacements for Glu-325, a residue that plays a direct role in H<sup>+</sup> translocation. These observations lend strong support for the argument that Arg-302 interacts with Glu-325 to facilitate deprotonation of the carboxylic acid during turnover.**

Lactose permease (lac permease), the product of the *lacY* gene (1), transduces free energy stored in an electrochemical H<sup>+</sup> gradient into a sugar concentration gradient by catalyzing the coupled stoichiometric translocation of galactosides and H<sup>+</sup> (lactose/H<sup>+</sup> symport; refs. 2 and 3). In the absence of substrate, lac permease does not translocate H<sup>+</sup>, and a substrate concentration gradient in itself generates a H<sup>+</sup> electrochemical gradient, indicating that the primary trigger for turnover is the binding and dissociation of substrate on opposite sides of the membrane. Site-directed mutagenesis of wild-type permease and complete Cys-scanning mutagenesis of a functional mutant devoid of Cys residues have allowed the delineation of functionally important amino acids (4). Furthermore, the application of a battery of site-directed methods to an extensive library of mutants has led to a structure at the level of helix packing, as well as dynamic information to help unravel the transport mechanism (5). Of the 417 residues in lac permease, only six side chains are irreplaceable for active transport. Glu-126 (helix IV) and Arg-144 (helix V) are directly involved in substrate binding and specificity (6–9). Furthermore, the two residues form a salt bridge (7, 10, 11). In contrast, Glu-269 (helix VIII), Arg-302 (helix IX), His-322 (helix X), and Glu-325 (helix X) are involved in H<sup>+</sup> translocation and/or coupling between H<sup>+</sup> and substrate translocation (12). In addition, Glu-269, Arg-302, His-322, and Glu-325 are in close proximity to (Fig. 1) and at about the same depth in the membrane as the major components of the substrate-binding site, Glu-126, Arg-144, and Cys-148 (5).

Recently, a mechanistic model for lactose/H<sup>+</sup> symport was postulated that describes the interactions between the irreplaceable side chains during permease turnover (13). In the ground state (Fig. 1), the permease is protonated, the H<sup>+</sup> is shared

between His-322 and Glu-269, and Glu-325 is charge-paired with Arg-302. In this conformation, which is the lowest free-energy state of the protein,<sup>†</sup> the permease binds ligand at the interface between helices IV (Glu-126) and V (Arg-144) at the outer surface of the membrane. Substrate binding induces a conformational change that leads to transfer of the H<sup>+</sup> from His-322–Glu-269 to Glu-325 and to reorientation of the binding site to the inner surface with release of sugar. Glu-325 is deprotonated on the inside because of rejuxtapositioning with Arg-302 as the conformation relaxes, and the His-322–Glu-269 complex is reprotonated from the outside surface to reinitiate the cycle.

The model explicitly predicts that the permease must be protonated to bind ligand with high affinity in the ground state and that His-322 and Glu-269 form the site of protonation. Evidence for this notion was obtained from a recent study (13) that determined the relationship between substrate affinity and the protonation state of the residues directly involved in H<sup>+</sup> translocation and/or coupling between sugar and H<sup>+</sup> translocation. Thus, the effect of pH on the binding of  $\beta$ ,D-galactopyranosyl 1-thio- $\beta$ ,D-galactopyranoside (TDG) was examined in single-Cys-148 permease (with or without conservative or neutral replacements for Glu-325, Arg-302, His-322, or Glu-269) by using a unique binding assay in which substrate protection of Cys-148 against alkylation by *N*-ethylmaleimide (NEM) is quantified (8, 9, 14). By this means, affinities ranging from submicromolar to high millimolar can be measured accurately. The results demonstrate that the ligand-binding affinity of single-Cys-148 permease mutants with Glu-325 (Asp or Gln) or Arg-302 replacements (Lys or Ala) is markedly decreased at alkaline pH, exhibiting a pK<sub>a</sub> of 8–9, whereas a Glu-269 replacement with Asp or His-322 replacements (Ala, Asn, or Gln) show essentially no change in binding affinity as a function of pH. Because the apparent pK<sub>a</sub> is significantly higher than the pK<sub>a</sub> of an unperturbed imidazole, we concluded that the H<sup>+</sup> is shared between His-322 and Glu-269 (Fig. 1), thereby raising the pK<sub>a</sub>.

Another important prediction of the model with respect to H<sup>+</sup> translocation is that upon substrate binding, the Glu-269–His-322 and Arg-302–Glu-325 pairs are disrupted, and the H<sup>+</sup> is transferred to Glu-325. After the substrate dissociates, the

Abbreviations: lac permease, lactose permease; TDG,  $\beta$ ,D-galactopyranosyl 1-thio- $\beta$ ,D-galactopyranoside; NEM, *N*-ethylmaleimide; KP<sub>i</sub>, potassium phosphate; NPG, *p*-nitrophenyl  $\alpha$ -D-galactopyranoside; RSO vesicles, right-side-out vesicles; CCCP, carbonylcyanide-*m*-chlorophenylhydrazone.

\*To whom reprint requests should be addressed at: Howard Hughes Medical Institute/University of California at Los Angeles, 5-748 MacDonald Research Laboratories, Box 951662, Los Angeles, CA 90095-1662. E-mail: RonaldK@HHMI.UCLA.edu.

<sup>†</sup>Deenergized right-side-out (RSO) membrane vesicles containing lac permease or purified permease in dodecyl- $\beta$ ,D-maltopyranoside bind ligand with high affinity, indicating that the protonated, high-affinity conformation of the permease represents the conformation with the lowest free energy.

The publication costs of this article were defrayed in part by page charge payment. This article must therefore be hereby marked "advertisement" in accordance with 18 U.S.C. §1734 solely to indicate this fact.

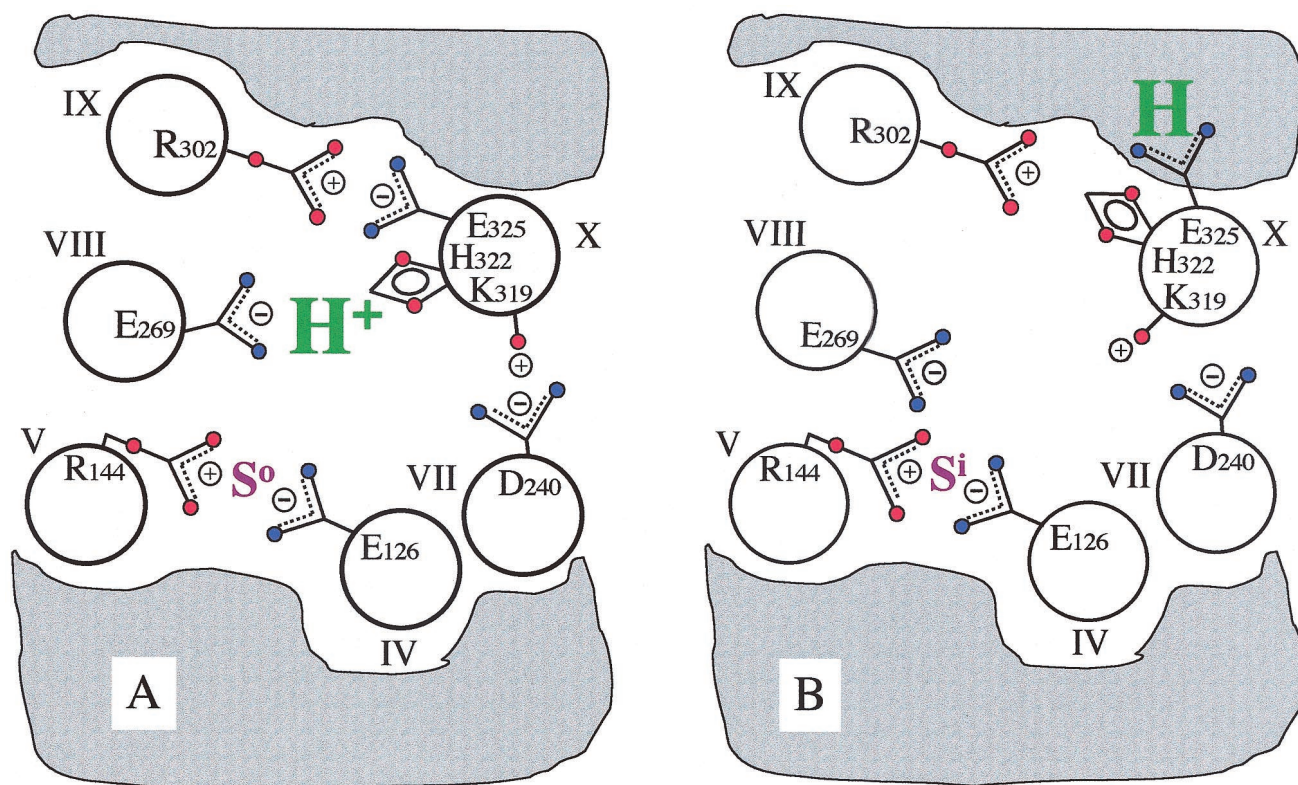


**Fig. 1.** Model for  $H^+$  translocation during lactose/ $H^+$  symport via lac permease. For clarity, 6 of the 12 helices that compose the permease are shown. The gray area designates the low dielectric environment of the lipid bilayer. (A) In the ground-state conformation, the relevant  $H^+$  is shared by His-322 (helix X) and Glu-269 (helix VIII), whereas Arg-302 (helix IX) is charge-paired with Glu-325 (helix X). In this conformation, lac permease binds substrate with high affinity at the outer surface ( $S^o$ ). Glu-126 (helix IV) and Arg-144 (helix V) are charge-paired and represent the major components of the substrate-binding site. Also shown is the charge-pair between Asp-240 (helix VII) and Lys-319 (helix X), which are not essential for the mechanism. (B) Substrate binding induces a conformational change that disrupts the E269/H322 and R302/E325 charge-pairs and leads to the transfer of the  $H^+$  to Glu-325, now stabilized by the low dielectric environment. At the same time, the substrate-binding site becomes exposed to the inner surface of the membrane ( $S^i$ ). After substrate dissociation, Glu-325 deprotonates at the inside surface (because of the re juxtaposition of Glu-325 with Arg-302) as the permease relaxes back to the ground-state conformation.

subsequent re juxtaposition between Arg-302 and Glu-325 is thought to be the primary driving force for deprotonation of the carboxylic acid as the protein relaxes back to the ground-state conformation. Evidence supporting this contention comes from previous observations demonstrating that lac permease mutants with neutral replacements for Glu-325 are specifically defective in all translocation modes that involve net  $H^+$  movement (active lactose accumulation, as well as influx or efflux down a concentration gradient) but bind ligand and catalyze equilibrium exchange and counterflow as well as or better than wild type (15–17, 30). Therefore, Glu-325 must play a direct role in  $H^+$  translocation.

A variety of structural studies places the Arg-302 residue in close proximity to Glu-325 (18–20), leading to the idea that the interaction is essential for controlling the protonation state of Glu-325 and is responsible for deprotonation during turnover. Consequently, it would be anticipated that neutral replacements for Arg-302 or Glu-325 should result in similar phenotypes. However, the Arg-302 mutants studied thus far do not exhibit the properties expected. When Arg-302 is replaced with Leu, the permease is defective in all translocation modes, as well as ligand binding, although “downhill” influx of lactose at high substrate concentrations without  $H^+$  translocation is observed (21, 22). Surprisingly, even the conservative Lys replacement is completely inactive (L. Patel, M.S.-T., and H.R.K., unpublished observations). On the other hand, mutants R302S and R302H possess a marginal ability to accu-

mulate lactose and catalyze sugar-dependent  $H^+$  influx (22). To reexamine the proposed role of Arg-302, the transport properties of mutants R302A and R302S were analyzed in this study. These mutants were selected because unlike R302K (13), both mutants bind ligand with high affinity. The results demonstrate that R302A or R302S permease exhibits properties analogous to mutants with neutral replacements for Glu-325, indicating that a guanidino group at position 302 is critical for efficient deprotonation of the carboxylic acid at position 325 during permease turnover.

#### Experimental Procedures

**Construction of Mutants.** Mutants E325A, R302A, and R302S were constructed by overlap-extension PCR mutagenesis and cloned into the expression vector pT7-5/lacY by using *Kpn*I and *Spe*I restriction sites.

**Growth of Cells and Preparation of RSO Membrane Vesicles.** *Escherichia coli* T184 harboring given mutants were grown in Luria-Bertani medium with ampicillin (100  $\mu$ g/ml). Fully grown cultures were diluted 10-fold and allowed to grow for 2 h at 37°C before induction with 1 mM *i*-propyl 1-thio- $\beta$ -D-galactopyranoside. After additional growth for 2 h at 37°C, cells were harvested by centrifugation. RSO membrane vesicles were prepared as described (23, 24) and resuspended in 100 mM potassium phosphate (KPi; pH 7.5) at a protein concentration of 32 mg/ml, frozen in liquid  $N_2$ , and stored at  $-80^\circ\text{C}$  until use.

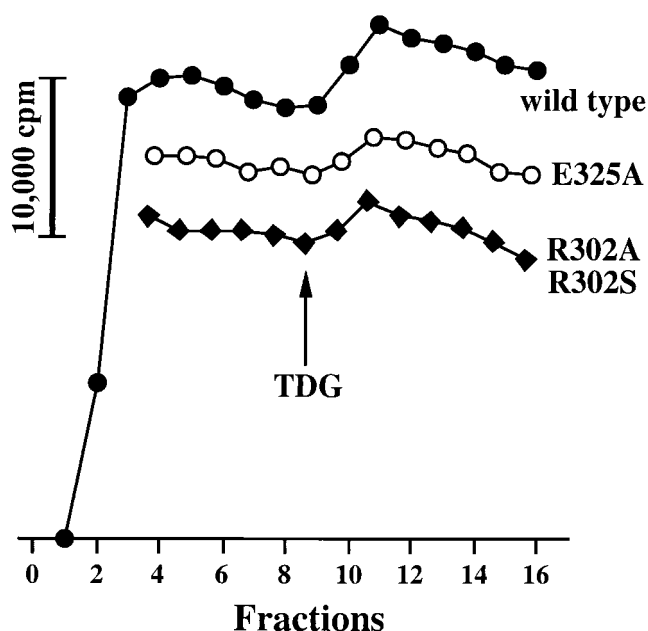


**Fig. 2.** Binding of NPG to RSO membrane vesicles. Binding of [ $^3\text{H}$ ]NPG to nonenergized RSO vesicles was assayed by flow dialysis as described in *Experimental Procedures*. An aliquot of RSO vesicles (250  $\mu\text{l}$ ) in 0.1 M  $\text{KPi}$  (pH 7.5) at a protein concentration of 32 mg/ml was placed in the upper chamber. [ $^3\text{H}$ ]NPG (4  $\mu\text{l}$ ; 0.95 mCi/mmol;  $\approx 4 \times 10^6$  cpm) was added to a final concentration of 16  $\mu\text{M}$  at fraction 1. As indicated by the arrow, 2.5  $\mu\text{l}$  of TDG was added to the upper chamber to a final concentration of 10 mM. For clarity, curves are displayed in decreasing order; however, the actual levels of radioactivity in the dialysate were identical in fractions 1 through 9 in each case (i.e., the curves should be superimposed).

**Flow Dialysis.** Binding of [6- $^3\text{H}$ ] p-nitrophenyl  $\alpha$ -D-galactopyranoside (NPG) (kindly provided by Gérard LeBlanc, Laboratoire J. Maetz/Commissariat à l'Énergie Atomique, Ville Franche-sur-Mer, France) was measured by flow dialysis as described (8, 25). The upper chamber contained 250  $\mu\text{l}$  of RSO vesicles in 0.1 M  $\text{KPi}$  (pH 7.5) under constant stirring at a protein concentration of 32 mg/ml. To ensure complete deenergization, 20  $\mu\text{M}$  valinomycin and 0.4  $\mu\text{M}$  nigericin (final concentrations) were added to the vesicles in the upper chamber. Buffer [0.1 M  $\text{KPi}$  (pH 7.5)] was pumped through the lower chamber at a flow rate of 0.5 ml/min, and 1-ml fractions were collected. Aliquots (0.9 ml) were assayed for radioactivity by addition of 5 ml of ScintiSafe Econo 2 (Fisher Scientific) scintillation mixture and liquid scintillation spectrometry.

**Transport Assays.** For active transport, *E. coli* T184 was washed once with 100 mM  $\text{KPi}$ , pH 7.5/10 mM  $\text{MgSO}_4$  and adjusted to an optical density of 10.0 at 600 nm (0.7 mg of protein per ml). Transport was initiated by the addition of [ $^1\text{-}^{14}\text{C}$ ]lactose [10 mCi/mmol specific activity (1 Ci = 37 GBq), 0.4 mM final concentration]; samples were quenched at given times by 100 mM  $\text{KPi}$ , pH 5.5/100 mM LiCl and assayed by rapid filtration (23, 26).

Downhill lactose influx in *E. coli* HB101 ( $\text{lacZ}^+\text{Y}^-$ ) was measured under similar conditions, with the exception that 20  $\mu\text{M}$  (final concentration) carbonylcyanide-*m*-chlorophenylhydrazone (CCCP) was included to deenergize the cells.

Efflux and equilibrium exchange were carried out with RSO vesicles as described (8, 17, 27). Vesicles were washed with 100 mM  $\text{KPi}$  (pH 7.5) and resuspended in the same buffer at a protein concentration of 32 mg/ml. [ $^1\text{-}^{14}\text{C}$ ]Lactose (10 mCi/

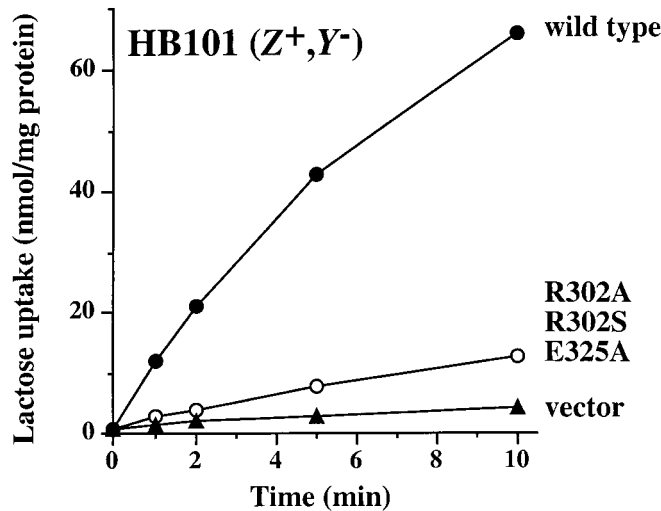
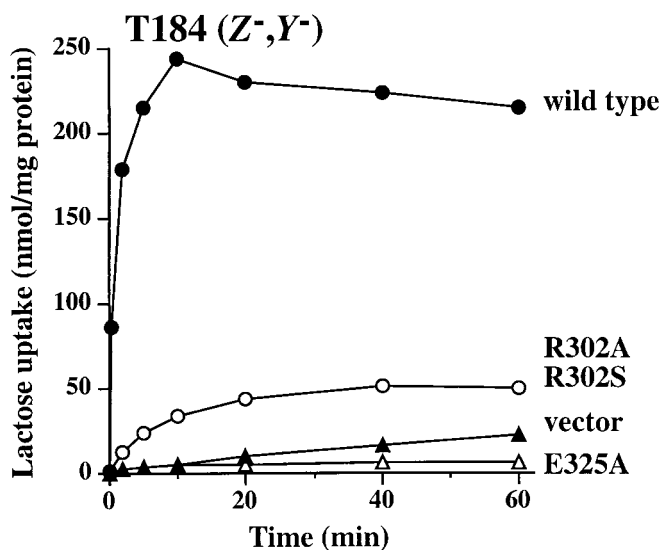


**Fig. 3.** Time courses of active lactose transport by *E. coli* T184 ( $\text{Z}^-\text{Y}^-$ ) or downhill lactose translocation by *E. coli* HB101 ( $\text{Z}^+\text{Y}^-$ ) expressing wild-type permease, mutants R302A and R302S, no permease (pT7-5 vector only), or mutant E325A. Cells were grown at 37°C, and aliquots of cell suspensions (50  $\mu\text{l}$ , containing  $\approx 35$   $\mu\text{g}$  of protein in 100 mM  $\text{KPi}$ , pH 7.5/10 mM  $\text{MgSO}_4$ ) were assayed at 0.4 mM final external lactose concentrations as described in *Experimental Procedures*. For downhill assays with *E. coli* HB101, 20  $\mu\text{M}$  CCCP was included to abolish the  $\text{H}^+$  electrochemical gradient.

mmol specific activity; 10 mM final concentration) was added, and equilibration was accomplished by incubating the samples at 4°C overnight in the presence of valinomycin (50  $\mu\text{M}$ ) and nigericin (0.5  $\mu\text{M}$ ). To initiate efflux or exchange, aliquots (2  $\mu\text{l}$ ) were rapidly diluted into 0.4 ml (200-fold) of 100 mM  $\text{KPi}$  (pH 7.5) containing 10 mM nonradioactive lactose (exchange) or no lactose (efflux). Reactions were quenched at given times with 100 mM  $\text{KPi}$ , pH 5.5/100 mM LiCl and assayed by rapid filtration.

## Results

**Direct Binding Assays.** To obtain direct evidence that mutants in Arg-302 bind substrate with relatively high affinity, RSO membrane vesicles containing wild-type, R302A, or R302S permease

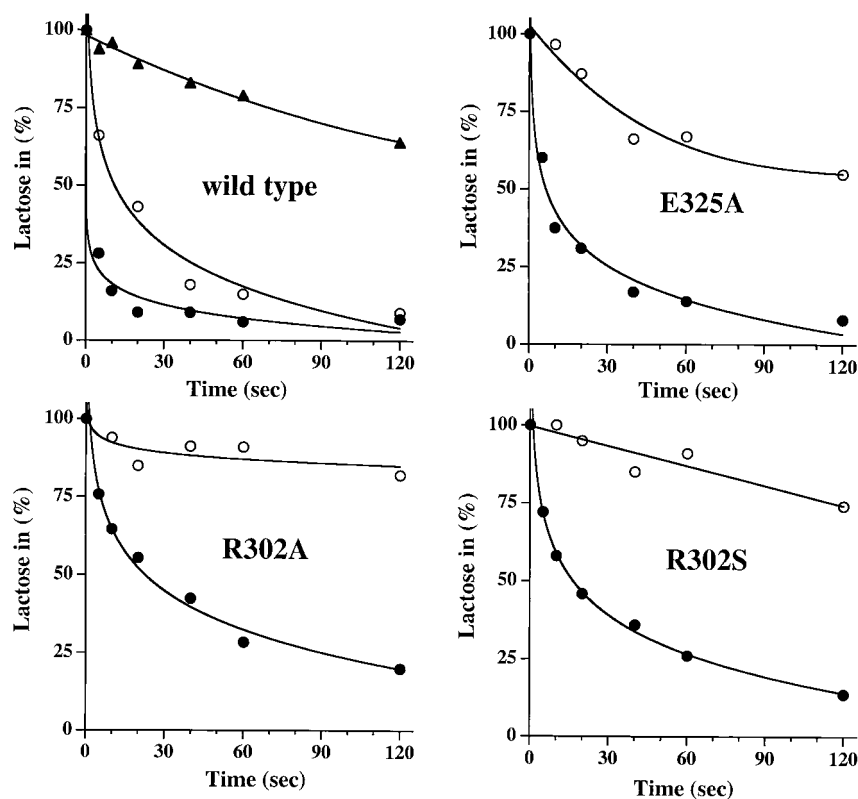


**Fig. 4.** Lactose efflux and equilibrium exchange by RSO membrane vesicles containing wild-type permease, E325A, R302A, and R302S permease mutants. RSO vesicles were equilibrated with 10 mM [ $1\text{-}^{14}\text{C}$ ]lactose (pH 7.5) and assayed by dilution into equilibration buffer without lactose (efflux; open circles) or with 10 mM lactose (exchange; solid circles) as described in *Experimental Procedures*. Nonspecific, passive lactose efflux was assayed after NEM treatment and is shown only for wild-type permease (solid triangles). Although not shown, the loss of radioactivity from NEM-treated vesicles containing E325A, R302A, or R302S permease was identical to the permease-mediated efflux activity of these mutants (i.e., coincides with the empty circles).

were assayed for binding of the high-affinity ligand NPG by flow dialysis under nonenergized conditions (Fig. 2). At the inception of the experiments, [ $^3\text{H}$ ]NPG was added to the upper chamber containing membrane vesicles; radioactivity in the dialysate increased linearly (fractions 1–3), reached a maximum (fractions 4–5), and then decreased at a slow rate. When a saturating concentration of TDG was added to the upper chamber (fraction 9), bound NPG was displaced, and the concentration of dialyzable radioactivity increased. Under these conditions, about 5,000 cpm displacement of NPG was observed with wild-type permease, whereas mutants E325A, R302A, or R302S exhibited displacements of about 2,500–3,000 cpm.

**Expression of Mutants.** Although results are not shown, mutants R302A and R302S exhibit expression levels in the membrane that are identical to those of wild-type or E325A permease, as determined by Western blot analyses.

**Active Transport and Downhill Lactose Influx.** Active lactose accumulation driven by a  $\text{H}^+$  electrochemical gradient was assayed in *E. coli* T184 ( $\text{lacY}^- \text{Z}^-$ ). Mutants R302A and R302S accumulate lactose at a very low rate up to about 20% of wild type at steady-state (Fig. 3 *Upper*). In contrast, as shown in refs. 15–17, E325A permease does not catalyze any lactose accumulation whatsoever. Although data are not presented, lactose accumulation relative to wild type by R302A or R302S permease is similar at pH 5.5 and pH 8.5, whereas E325A is inactive at any pH tested.

Lactose influx down a concentration gradient occurs in symport with  $\text{H}^+$ . To assess the ability of the mutants to catalyze downhill lactose influx, *E. coli* HB101 ( $\text{lacY}^- \text{Z}^+$ ) was transformed with appropriate plasmids, and rates of uptake were measured under deenergized conditions in the presence of the protonophore CCCP. Because lactose taken up is immediately degraded by cytoplasmic  $\beta$ -galactosidase, an inward lactose concentration gradient is maintained throughout the assay. As shown in Fig. 3 *Lower*, mutants R302A and R302S are as defective as E325A permease, and lactose uptake exceeds passive lactose influx only marginally, as observed in cells carrying no *lacY* gene.

**Efflux and Equilibrium Exchange.** Lactose efflux down a concentration gradient is permease-mediated and occurs in symport with  $\text{H}^+$ . In contrast, equilibrium exchange does not involve net  $\text{H}^+$  translocation; the permease recycles in the protonated state (see ref. 28). When RSO membrane vesicles containing wild-type permease are equilibrated with 10 mM [ $1\text{-}^{14}\text{C}$ ]lactose and diluted into medium devoid of lactose (efflux) or into medium containing 10 mM unlabeled lactose (equilibrium exchange), a loss of intravesicular radioactivity occurs, and the rate of efflux is slower than the rate of exchange ( $t_{1/2} = \approx 2\text{--}4$  s for exchange and 10–15 s for efflux; Fig. 4; refs. 27 and 29). Pretreatment of the vesicles with NEM (a sulfhydryl reagent that inactivates the permease) abolishes permease-mediated efflux and exchange, and only passive loss of lactose from the vesicles is observed. In contrast to wild type, vesicles containing E325A permease are markedly defective with respect to efflux but catalyze normal

exchange ( $t_{1/2} = \approx 6$  s), as shown (15–17). Efflux observed with mutant E325A is not carrier-mediated, because vesicles with E325A permease treated with NEM exhibit the same rate of lactose efflux. Mutants R302A and R302S exhibit essentially identical patterns to those of E325A. Both mutants are completely defective with respect to efflux ( $t_{1/2} = \gg 2$  min) but catalyze equilibrium exchange at highly significant rates, albeit somewhat slower than those of wild-type or E325A permease ( $t_{1/2} = \approx 15$ –20 s).

## Discussion

The present study provides strong evidence that the major role of Arg-302 in the catalytic mechanism of lac permease is to facilitate deprotonation of Glu-325 during lactose/ $H^+$  symport. Thus, mutants R302A and R302S are specifically defective in translocation reactions that involve  $H^+$  translocation—accumulation of the disaccharide against a concentration gradient, as well as downhill lactose influx and efflux—but bind ligand and catalyze equilibrium exchange. Importantly, these transport properties are highly analogous to those of neutral replacement mutants in Glu-325 (which participates directly in  $H^+$  translocation). Thus, mutations at Arg-302 exert their effects through interactions with Glu-325. The present observations stand in contrast with other studies indicating that mutant R302L is completely defective in all transport modes, including exchange (21, 22). However, this mutant does not bind NPG (21). The present study uses two less bulky replacements, Ala and Ser, and in both cases ligand binding is preserved, suggesting that these side chains do not perturb the Glu-269–His-322 interaction, unlike the branched hydrophobic side chain of Leu. It is also noteworthy that there is no discernible difference between the properties of R302A and R302S, indicating that side-chain bulk, rather than hydrophobicity, is important in determining the effects of Arg-302 replacements.

A remarkable feature of the Arg-302–Glu-325 mutants is that the defect in the  $H^+$ -coupled translocation modes is completely symmetric; both efflux and influx (or active accumulation) are equally affected. This and other considerations suggest that influx and efflux are functionally symmetric processes, a notion that is not readily apparent, given the asymmetric arrangement of the participating side chains and the vectorial nature of  $H^+$  translocation (see Fig. 1). Permease turnover during lactose influx down a concentration gradient or active lactose accumulation can be explained by a simple kinetic scheme that consists of six steps (Fig. 5): (i) protonation of the permease from the outer surface of the membrane at His-322–Glu-269; (ii) binding of lactose to the permease at the outer surface of the membrane; (iii) a conformational change in the permease that results in translocation of the ternary complex to the inner surface of the membrane, with the sugar-binding site facing inside and the  $H^+$  transferred from Glu-269–His-322 to Glu-325; (iv) release of substrate on the inner surface; (v) release of  $H^+$  from Glu-325 at the inner surface; and (vi) a conformational change corresponding to the return of the unloaded permease to the outer surface of the membrane. As discussed above, mutants in both Arg-302 and

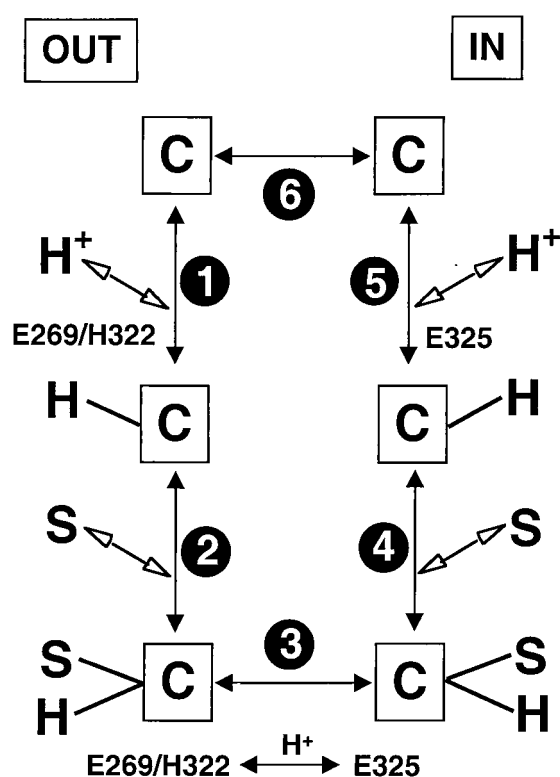


**Fig. 5.** Six-step kinetic model describing lactose influx or active transport. Also indicated are the steps at which residues Glu-269, His-322, and Glu-325 are thought to be involved. See text for details. C, lac permease;  $H^+$ , transported proton; S, transported sugar.

Glu-325 are defective in step v, indicating that the residues are critical for deprotonation of the permease during influx. Lactose efflux down a concentration gradient can be explained with the same six steps. However, in this case, the process is initiated at the inner surface of the membrane, and the cycle is driven backwards by the lactose concentration gradient as a result of mass action and the tendency of the permease to return to its lowest free-energy conformation. Consequently, protonation of the permease first takes place at Glu-325, and substrate binding induces  $H^+$  transfer to Glu-269–His-322. Therefore, under efflux conditions, the primary role of Arg-302 is to facilitate deprotonation of Glu-325 toward Glu-269–His-322. Substrate dissociation at the outer surface is driven by the concentration gradient, whereas deprotonation of His-322–Glu-269 to the outside is caused by the inherent cooperativity between  $H^+$  and substrate binding.

We thank Adam Weinglass for stimulating discussions and help with the artwork and Wei Zhang for providing RSO vesicles. This work was supported in part by National Institutes of Health Grant DK51131 (to H.R.K.).

- Müller-Hill, B. (1996) *The lac Operon: A Short History of a Genetic Paradigm* (de Gruyter, New York).
- Kaback, H. R. (1976) *J. Cell. Physiol.* **89**, 575–593.
- Kaback, H. R. (1983) *J. Membr. Biol.* **76**, 95–112.
- Frillingos, S., Sahin-Tóth, M., Wu, J. & Kaback, H. R. (1998) *FASEB J.* **12**, 1281–1299.
- Kaback, H. R. & Wu, J. (1999) *Acc. Chem. Res.* **32**, 805–813.
- Frillingos, S., Gonzalez, A. & Kaback, H. R. (1997) *Biochemistry* **36**, 14284–14290.
- Venkatesan, P. & Kaback, H. R. (1998) *Proc. Natl. Acad. Sci. USA* **95**, 9802–9807.

- Sahin-Tóth, M., le Coutre, J., Kharabi, D., le Maire, G., Lee, J. C. & Kaback, H. R. (1999) *Biochemistry* **38**, 813–819.
- Sahin-Tóth, M., Akhoun, K. M., Runner, J. & Kaback, H. R. (2000) *Biochemistry* **39**, 5907–5103.
- Zhao, M., Zen, K.-C., Hubbell, W. & Kaback, H. R. (1999) *Biochemistry* **38**, 7407–7412.
- Wolin, C. D. & Kaback, H. R. (2000) *Biochemistry* **39**, 6130–6135.
- Kaback, H. R. (1997) *Proc. Natl. Acad. Sci. USA* **94**, 5539–5543.
- Sahin-Tóth, M., Karlin, A. & Kaback, H. R. (2000) *Proc. Natl. Acad. Sci. USA* **97**, 10729–10732. (First Published September 12, 2000; 10.1073/pnas.200351797)

14. Frillingos, S. & Kaback, H. R. (1996) *Biochemistry* **35**, 3950–3956.
15. Carrasco, N., Antes, L. M., Poonian, M. S. & Kaback, H. R. (1986) *Biochemistry* **25**, 4486–4488.
16. Carrasco, N., Puttner, I. B., Antes, L. M., Lee, J. A., Larigan, J. D., Lolkema, J. S., Roepe, P. D. & Kaback, H. R. (1989) *Biochemistry* **28**, 2533–2539.
17. Frillingos, S. & Kaback, H. R. (1996) *Biochemistry* **35**, 10166–10171.
18. Jung, K., Jung, H., Wu, J., Privé, G. G. & Kaback, H. R. (1993) *Biochemistry* **32**, 12273–12278.
19. He, M., Voss, J., Hubbell, W. L. & Kaback, H. R. (1997) *Biochemistry* **36**, 13682–13687.
20. He, M. M., Voss, J., Hubbell, W. L. & Kaback, H. R. (1995) *Biochemistry* **34**, 15667–15670.
21. Menick, D. R., Carrasco, N., Antes, L. M., Patel, L. & Kaback, H. R. (1987) *Biochemistry* **26**, 6638–6644.
22. Matzke, E. A., Stephenson, L. J. & Brooker, R. J. (1992) *J. Biol. Chem.* **267**, 19095–19100.
23. Kaback, H. R. (1974) *Methods Enzymol.* **31**, 698–709.
24. Short, S. A., White, D. C. & Kaback, H. R. (1972) *J. Biol. Chem.* **247**, 7452–7458.
25. Rudnick, G., Schuldiner, S. & Kaback, H. R. (1976) *Biochemistry* **15**, 5126–5131.
26. Kaback, H. R. (1971) *Methods Enzymol.* **22**, 99–120.
27. Kaczorowski, G. J. & Kaback, H. R. (1979) *Biochemistry* **18**, 3691–3697.
28. Zhang, W. & Kaback, H. R. (2000) *Biochemistry* **47**, 14538–14542.
29. Kaczorowski, G. J., Robertson, D. E. & Kaback, H. R. (1979) *Biochemistry* **18**, 3697–3704.
30. Weinglass, A. B., Smirnova, I. N. & Kaback, H. R. (2001) *Biochemistry* **40**, 769–776.